

# Supporting Information

## New Insights into the Origins of Sb-Induced Effects on Self-Catalyzed GaAsSb Nanowire Arrays

*Dingding Ren,<sup>†</sup> Dasa L. Dheeraj,<sup>‡</sup> Chengjun Jin,<sup>†</sup> Julie S. Nilsen,<sup>§</sup> Junghwan Huh,<sup>†</sup>  
Johannes F. Reinertsen,<sup>†</sup> A. Mazid Munshi,<sup>‡</sup> Anders Gustafsson,<sup>¶</sup> Antonius T. J. van Helvoort,<sup>§</sup>  
Helge Weman,<sup>†,‡</sup> and Bjørn-Ove Fimland<sup>\*,†,‡</sup>*

<sup>†</sup> Department of Electronics and Telecommunications, Norwegian University of Science and  
Technology (NTNU), NO-7491 Trondheim, Norway

<sup>‡</sup> CrayoNano AS, Otto Nielsens vei 12, NO-7052 Trondheim, Norway

<sup>†</sup> Center for Atomic-scale Materials Design, Department of Physics, Technical University of  
Denmark, DK-2800 Kongens Lyngby, Denmark

<sup>§</sup> Department of Physics, Norwegian University of Science and Technology (NTNU), NO-7491  
Trondheim, Norway

<sup>¶</sup> Solid State Physics and NanoLund, Lund University, Box 118, SE-22100 Lund, Sweden

## S1. Summary of growth information for nanowire samples.

Table S1. Detailed growth information for the grown nanowire samples (Ga flux is 0.7 ML/s for the nanowire axial growth)

Sample	Series	Growth temp (°C)	Growth duration (min)	As <sub>2</sub> flux (Torr)	Sb <sub>2</sub> flux (Torr)	Patterning method and comments
A	Variant Sb flux series	625	35	$2.5 \times 10^{-6}$	$2 \times 10^{-7}$	NIL
B	Variant Sb flux series	625	35	$2.5 \times 10^{-6}$	$4 \times 10^{-7}$	NIL
C	Variant Sb flux series	625	35	$2.5 \times 10^{-6}$	$6 \times 10^{-7}$	NIL
D	Variant Sb flux series	625	35	$2.5 \times 10^{-6}$	$8 \times 10^{-7}$	NIL
E	Time series	625	10	$2.5 \times 10^{-6}$	$6 \times 10^{-7}$	NIL
F	Time series	625	20	$2.5 \times 10^{-6}$	$6 \times 10^{-7}$	NIL
G	Time series	625	35	$2.5 \times 10^{-6}$	$6 \times 10^{-7}$	NIL
H	Time series	625	45	$2.5 \times 10^{-6}$	$6 \times 10^{-7}$	NIL
I	Time series	625	60	$2.5 \times 10^{-6}$	$6 \times 10^{-7}$	NIL
J	Elevated temp	640	35	$2.5 \times 10^{-6}$	$6 \times 10^{-7}$	NIL
K	Various pitches	625	35	$2.5 \times 10^{-6}$	$4 \times 10^{-7}$	EBL and square-pattern with pitch length of 0.7, 1, 1.5 and 2 $\mu\text{m}$
L	Crystal phase	625	5	$4 \times 10^{-6}$	$4 \times 10^{-7}$	NIL
M	Optical series	625	35	$3 \times 10^{-6}$	0	NIL and Al <sub>0.3</sub> Ga <sub>0.7</sub> As shell
N	Optical series	625	35	$2.5 \times 10^{-6}$	$1 \times 10^{-7}$	NIL and Al <sub>0.3</sub> Ga <sub>0.7</sub> As shell
O	Optical series	625	35	$2.5 \times 10^{-6}$	$2 \times 10^{-7}$	NIL and Al <sub>0.3</sub> Ga <sub>0.7</sub> As shell

AlGaAs/GaAs shell growth details:

In order to passivate the GaAsSb nanowire surface states for the PL and CL measurements, samples M, N and O were grown with a radial Al<sub>0.3</sub>Ga<sub>0.7</sub>As (nominal composition) shell of 14 nm and GaAs cap of 6 nm consecutively at 625 °C after solidification of the Ga catalyst. The Al<sub>0.3</sub>Ga<sub>0.7</sub>As shell was grown under an Al flux of 0.1 ML/s, a Ga flux of 0.2 ML/s and an As<sub>2</sub> flux of  $8 \times 10^{-6}$  Torr for 30 min; then the GaAs cap was grown under a Ga flux of 0.3 ML/s and an As<sub>2</sub> flux of  $8 \times 10^{-6}$  Torr for 12 min.

Energy-dispersive X-ray spectroscopy (EDX) characterization:

The Sb composition of samples A to D were measured by energy-dispersive X-ray spectroscopy at nanowire position  $\sim 500$  nm below the droplets, and their nominal Sb compositions (from averaging several nanowires) were found to be 6%, 15%, 16%, and 19%, respectively.

### S2. Time series of GaAsSb nanowire arrays.

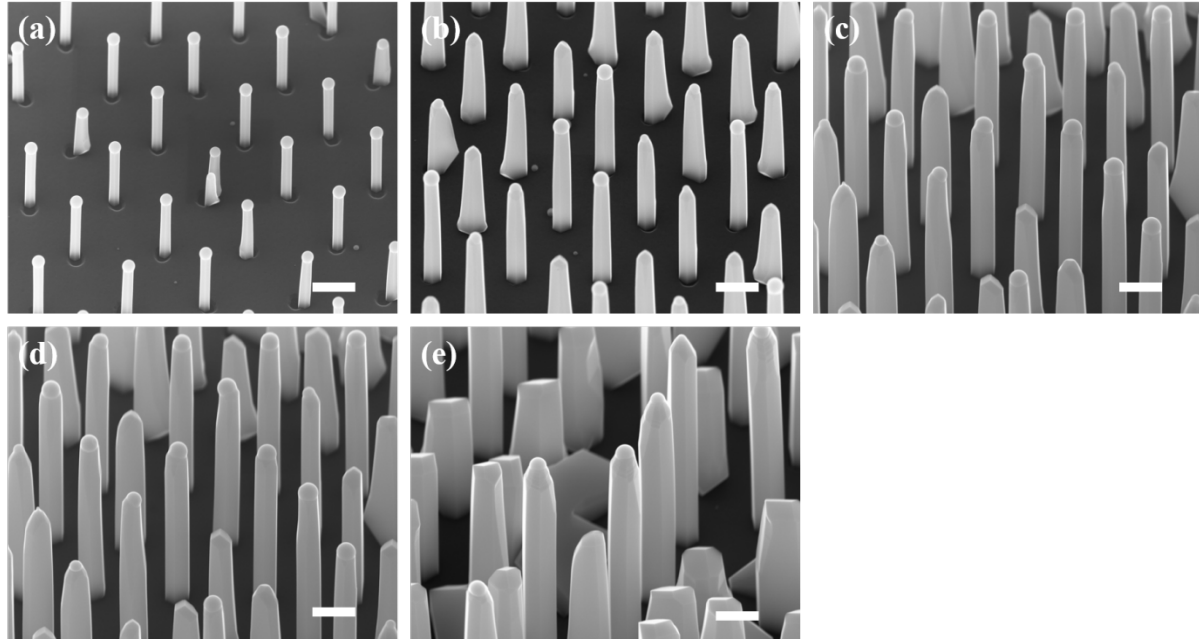


**Figure S1.** 45° tilted-view SEM images of GaAsSb nanowire arrays grown for (a) 10 min, (b) 20 min, (c) 35 min, (d) 45 min, and (e) 60 min under an  $\text{As}_2$  flux of  $2.5 \times 10^{-6}$  Torr, an  $\text{Sb}_2$  flux of  $6 \times 10^{-7}$  Torr, a Ga flux of 0.7 ML/s, and at a substrate temperature of 625 °C. Scale bars are 500 nm.

### S3. Computation methods of the density functional theory (DFT).

DFT calculations were performed in the GPAW electronic structure code using the projector-augmented wave method.<sup>1</sup> The wave functions are sampled on a grid and the Perdew–Burke–Ernzerh (PBE) exchange-correlation functional is employed.<sup>2</sup> All the structures are calculated based on zinc blende (ZB) structure and optimized until the force on each atom is smaller than 0.02 eV/Å.

### S3.1. Calculation of binding energy.

The binding energy of a Ga adatom on the GaAs(110) surface is defined as

$$E^b = E_{tot}[GaAs(110)] + E_{tot}[Ga] - E_{tot}[Ga@GaAs(110)]. \quad (S1)$$

The binding energy of a Ga adatom on the GaAs(110) surface where the Ga atom is also bonded to one Sb atom adsorbed on the GaAs(110) surface is defined as

$$E^b = E_{tot}[Sb \text{ adsorbed on } GaAs(110)] + E_{tot}[Ga] - E_{tot}[Ga@Sb \text{ adsorbed on } GaAs(110)]. \quad (S2)$$

Equation S2 will also apply if Sb is substituted with As. The presence of one Sb or As atom (in red in Figure S2-1) on the GaAs(110) surface results in an increase of the binding energy of an interacting Ga adatom on the surface from 2.01 eV to 2.34 eV and 2.60 eV, respectively. The schematic of Sb or As atom enhanced Ga binding to the GaAs(110) surface is shown in Figure S2-1.

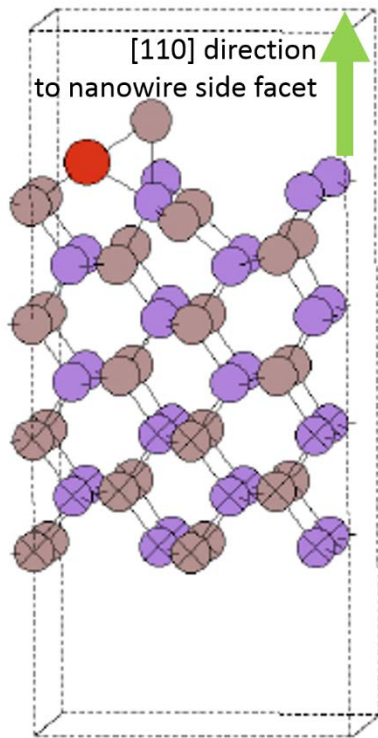


Figure S2-1. The atomic structure of Ga adsorbed on the ZB GaAs(110) surface with the presence of one adsorbed Sb or As atom (adsorbed Sb or As atom in red).

### S3.2. Calculation of chemical potential change by substitution of As with Sb, P or N.

As shown in Fig. S2-2, a  $2 \times 2 \times 2$  ZB GaAs supercell with one atom substituted by Sb are used to calculate the chemical potential change from GaAs. Thus, the chemical potential change by incorporation of Sb is defined as

$$E[Sb] = E_{tot}[Ga_{32}As_{31}Sb] - E_{tot}[Ga_{32}As_{32}], \quad (S3)$$

where  $E_{tot}[Ga_{32}As_{31}Sb]$  and  $E_{tot}[Ga_{32}As_{32}]$  denote the total energy of the substituted and perfect systems, respectively. The calculation of chemical potential change from substitution by P or N were also carried out the same way as for Sb.  $E[Sb]$ ,  $E[P]$  and  $E[N]$  were calculated to be 1.486 eV, -0.896 eV and -2.481 eV, respectively.

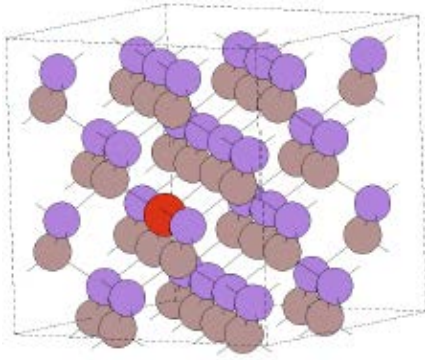
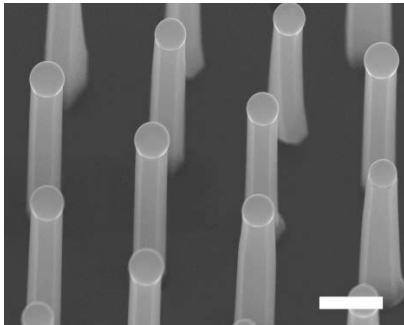


Figure S2-2. The atomic structure of a  $2 \times 2 \times 2$  ZB GaAs supercell with one Sb substitution (Sb atom in red).

### S4. GaAsSb nanowire array grown at an elevated temperature of 640 °C.



**Figure S3.** 30° tilted-view SEM image of a GaAsSb nanowire array grown at an elevated temperature of 640 °C (sample J). The scale bar is 500 nm.

### S5. Thermodynamic analysis based on GaAs-GaSb phase diagram.

The schematic of GaAs-GaSb pseudobinary liquidus and solidus plots are shown in figure S4.<sup>3</sup> At for example 900 °C, GaAs<sub>1-y</sub>Sb<sub>y</sub> will change from solid to solid-liquid mixture, and further to liquid by increasing the Sb composition under equilibrium condition, as indicated by the red dashed arrow. As supersaturation is defined by the chemical potential difference between liquid and solid phase, the changing from solid to liquid by composition modulation indicates a decreased supersaturation by changing the composition from GaAs to GaSb, that is, increasing the Sb composition. Although the phase diagram could represent the trend of chemical potential change at higher temperatures than a typical growth temperature for GaAsSb nanowires (e.g. 625 °C), the trend of supersaturation change should be similar at the growth temperature.

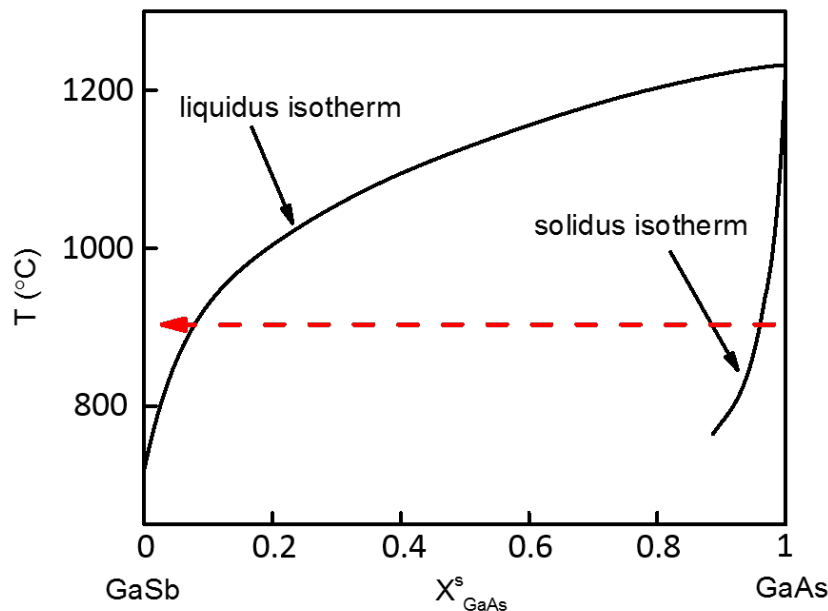


**Figure S4.** Schematic pseudobinary liquidus and solidus for GaAs-GaSb.<sup>3</sup>

### REFERENCES

- (1) Enkovaara, J.; Rostgaard, C.; Mortensen, J. J.; Chen, J.; Duřak, M.; Ferrighi, L.; Gavnholt, J.; Glinsvad, C.; Haikola, V.; Hansen, H. A.; Kristoffersen, H. H.; Kuisma, M.; Larsen, A. H.; Lehtovaara, L.; Ljungberg, M.; Lopez-Acevedo, O.; Moses, P. G.; Ojanen, J.; Olsen, T.; Petzold, V.; Romero, N. A.; Stausholm-Møller, J.; Strange, M.; Tritsarlis, G. A.; Vanin, M.; Walter, M.; Hammer, B.; Häkkinen, H.; Madsen, G. K. H.; Nieminen, R. M.; Nørskov, J. K.; Puska, M.; Rantala, T. T.; Schiøtz, J.; Thygesen, K. S.; Jacobsen, K. W. *J. Phys. Condens. Matter* **2010**, *22*, 253202.
- (2) Perdew, J. P.; Burke, K.; Ernzerhof, M. *Phys. Rev. Lett.* **1996**, *77*, 3865–3868.
- (3) Panish, M. B.; Ilegems, M. *Prog. Solid State Chem.* **1972**, *7*, 39–83.